

A 1 MV 9.5 MHz SYSTEM FOR THE CERN ANTIPROTON COLLECTOR

J. Boucheron, R. Garoby, D. Grier, M. Paoluzzi, F. Pedersen
PS Division, CERN, 1211 Geneva 23, Switzerland

Summary

A 1 MV 9.5 MHz rf system has been installed in the CERN Antiproton Collector (AC) to process the incoming antiproton bunches. The initial momentum spread (6%) is reduced by a factor 4 using bunch rotation followed by adiabatic debunching. Two capacitively loaded cavities of compact design are used. Each cavity is driven by a 700 kW pulsed rf generator using MOSFET cathode switches for bias switching in the final stage. Fast (50 μ s) cavity discharge is obtained by dissipating the stored energy back into the generator through a $\lambda/4$ feeder line. Closed loop control of the gap voltage and phase during the 100 μ s flat top and the adiabatic debunching ensures stable operation. The design principles and their implementation, as well as performances and operating experience are reported.

Introduction

The AC was designed to increase the accumulation rate of the existing Antiproton Accumulator (AA) by a factor ten [1]. A substantial part of that increase comes from the fourfold improvement of the momentum acceptance of the AC (6%) compared to that of the AA (1.5%).

A dedicated rf system for bunch rotation and adiabatic debunching is needed to reduce the momentum spread of the incoming bunches by a factor four, so that the longitudinal cooling system can take over. This technique has been preferred to adiabatic debunching immediately after injection, because it reduces the maximum required rf voltage by a factor 6-10 depending on initial bunch length.

The rf system requirements are (Fig. 1):

Frequency	9.537	MHz
Peak voltage during rotation	1.3	MV
Peak voltage for matching	130.0	kV
Rotation time	60.5	μ s
Fast discharge time	20.0	μ s
Adiabatic discharge time	10.0	ms
Repetition rate	2.4	s

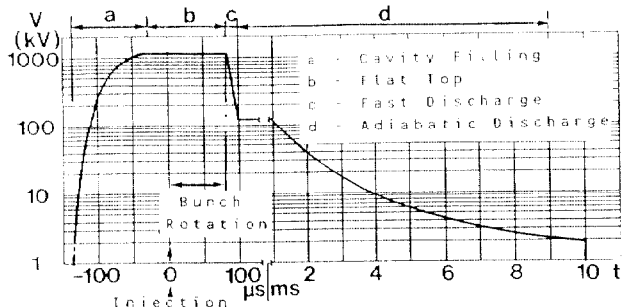


Fig. 1: Typical voltage program

The rf voltage is obtained using two independent cavities. Each cavity is driven by a 700 kW power stage through a 19 meters coaxial line. All the electronics (low and high power) are installed in the AAC hall, which is accessible while antiprotons are circulating in the AA ring but not during accumulation and ejection.

The Cavity

The cavity is shown in Figs. 2 and 3. Its dimensions were mainly dictated by the space available in the AC ring. To resonate the relatively small cavity volume at the working frequency, reactive loading is necessary. Because of the risk of exciting circumferential modes and of electrical breakdown [1], ferrite was avoided in favour of capacitive loading of the gap even though this choice undesirably decreases the cavity R/Q and therefore increases the stored energy.

The capacitive electrodes were designed to keep the maximum electric stress below the Kilpatrick limit, and to minimize the cavity detuning due to temperature and pressure variations. Fine tuning is achieved by adjusting the electrode spacing by means of a lever arm.

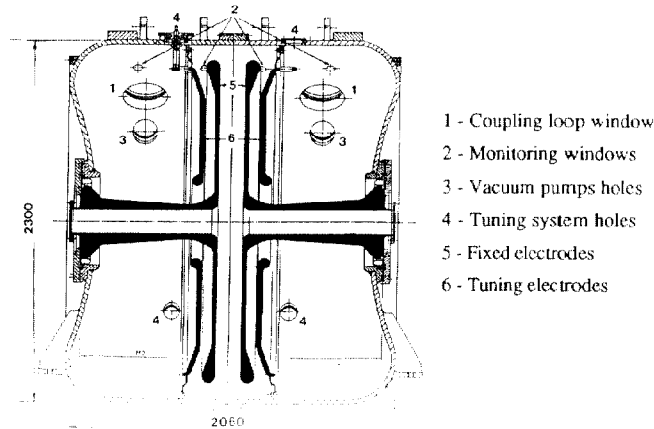


Fig. 2: Cavity cross-section.

In order to limit electrical losses whilst maintaining an acceptable weight and deformation under vacuum the cavity is specially shaped, and is constructed of Anticorodal W [2]. Since the duty cycle is low, no forced cooling is necessary. The strong coupling between the two halves of the cavity permits feeding from the coaxial line via a single loop. A conditioning time of about 1 day is necessary before the cavity voltage can be driven past the multipactoring region (~ 500 V) and up to full working voltage.

Parameters of the Cavity.

Parameter	Units	Cavity 1	Cavity 2
Resonant frequency	MHz	9.537	9.537
Quality factor (Measured)		7000	4500*
Quality factor (Superfish)		8300	8300
Geometry factor (R/Q)	Ω	39	39
Gap voltage	kV	650	520
Shunt impedance (R)	k Ω	275	175
Required power	kW	770	770
Equivalent C	pF	428	428
Equivalent L	nH	651	651
Time constant τ	μ s	235	150

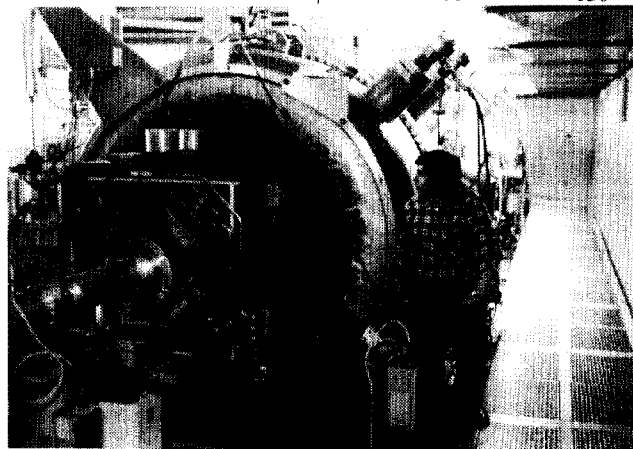


Fig. 3: Cavity in the AAC.

* Q factor of cavity 2 is lower because of a stainless-steel part mounted inside the cavity for vacuum reasons.

The rf Charge/Discharge Principle

A short cavity discharge time is essential for an efficient beam manipulation. The natural cavity discharge time of about 500 μ s has been shortened by using the properties of a $\lambda/4$ line in combination with the final tube as a crowbar to absorb the cavity stored energy during the discharge [3]. Referring to Fig. 4, the final tube is connected to the cavity coupling loop via a $\lambda/4$ line. The coupling between cavity and loop is represented by a transformer of ratio $N = V_c/V_s$; R is due to the cavity losses. When filling the cavity the tube acts as the final stage of the rf generator. At the end of cavity charge, with the cavity at resonance, the tube anode current is in phase with the driving voltage V_d (**), and counterphase to V_a . To maintain the voltage V_{c0} during the flat-top the tube has to deliver a power P_0 given by:

$$P_0 = \frac{V_{c0}^2}{2R} \tag{1}$$

For a $\lambda/4$ line $Z_0 = \frac{V_s}{I_a}$ or $Z_0 = \frac{V_c/N}{I_a}$ (2)

so that during the flat top the corresponding anode voltage and current can be expressed as

$$I_a = \frac{V_{c0}}{NZ_0} \tag{3}$$

and $V_a = \frac{V_{c0}}{R} NZ_0$ (4)

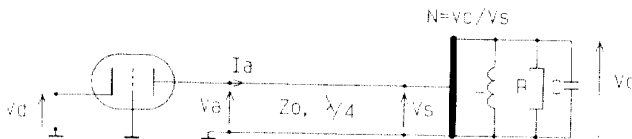


Fig. 4: Simplified equivalent circuit.

During the discharge the tube anode is driven by the cavity stored energy. To invert the direction of energy flow a fast reduction of V_d is sufficient (fast compared to the cavity τ). Due to the $\lambda/4$ line the anode voltage during discharge is in phase with the current and the tube behaves as a resistive load, adjustable by means of the driving voltage V_d . From Eq. (3), the power dissipated on the anode during the discharge is

$$P_a = \frac{V_a I_a}{2} = V_a' \frac{V_c}{2NZ_0} \tag{5}$$

where V_a' and I_a' are voltage and current during discharge.

The value of N is constrained by the voltage breakdown limit of the cavity loop vacuum window; the product NZ_0 in Eq. (3) is chosen so as not to exceed the maximum tube I_a at beginning of discharge. For a given NZ_0 the shortest discharge time is obtained when V_a' is kept at maximum during the whole discharge period. The anode current I_a' and the cavity voltage V_c then decrease linearly as shown in Fig. 5.

The energy lost by the cavity during the discharge time t_d is given by

$$\Delta W = \frac{C}{2} (V_{c0}^2 - V_c'^2) \tag{6}$$

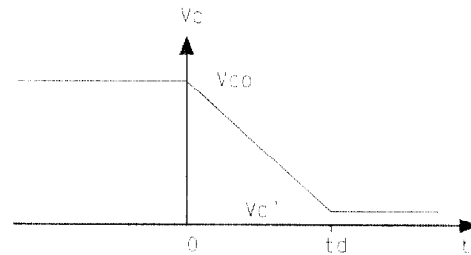


Fig. 5: Linear cavity discharge.

ΔW is the sum of the energy lost on the cavity itself (on R) and that dissipated by the tube. This can be expressed as

$$\Delta W = \int_0^{t_d} P_{r(t)} dt + \int_0^{t_d} P_{a(t)} dt \tag{7}$$

With constant V_a' during the discharge and noting that

$$V_{c(t)} = V_{c0} - \frac{V_{c0} - V_c'}{t_d} t \tag{8}$$

Equation 7 can be solved for t_d and gives

$$t_d = \frac{C}{2} \left(\frac{V_{c0}^2 - V_c'^2}{\left[V_a' (V_{c0} + V_c') / 4NZ_0 \right] + \left[(V_{c0}^2 + V_c'^2 + V_{c0} V_c') / 6R \right]} \right) \tag{9}$$

If the cavity natural discharge time is much longer than t_d , Eq. (9) simplifies to

$$t_d = \frac{2NZ_0 C}{V_a'} (V_{c0} - V_c') \tag{10}$$

Design and Development

With N set at 50 to give 13 kV at the cavity window, a Z_0 of 60 Ω gives an anode current I_a of 217 A and V_a of 7.1 kV at the end of cavity filling. From Eq. (10), a discharge time of 20 μ s requires a V_a' of 75 kV.

The final tube is a Thomson power triode type TH116 which has a V_a max of 75 kV and an I_a greater than 300 A (fundamental rf component). To avoid the need for a modulator to supply pulsed 10 kV anode voltage during operation, the tube is auto biased into cut-off by opening a power mosfet switch in the cathode circuit during the idle part of the cycle. This method allows the use of a simple dc power supply (Fig. 6) whose capacitors recharge during the tube cut-off period.

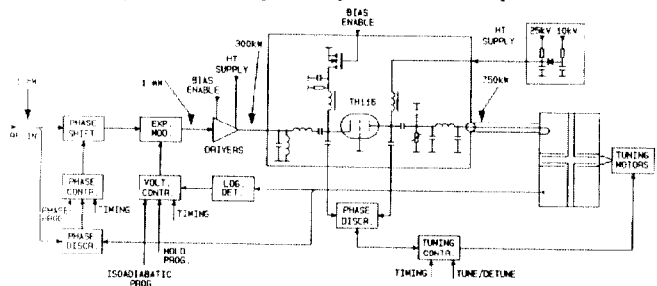


Fig. 6: Simplified system block diagram

The $\lambda/4$ transformer coupling the final amplifier to the cavity consists of a $\lambda/8$ π section L-C network in series with a $\lambda/8$ coaxial line. To cover the distance between the final tube and the cavity a further $\lambda/2$ coaxial line has been added. By tuning the elements in the

** Voltages and currents are fundamental peak envelope values. All time constants are assumed to be negligible compared to the cavity τ .

L-C π section located in the final amplifier, the $\lambda/4$ transformer electrical length and characteristic impedance can be adjusted.

The characteristic impedance of the $\lambda/8$ section is 60 Ω whilst that of the $\lambda/2$ line (16 Ω) has been chosen so as to minimize the VSWR on the line during the discharge (Fig. 7). Both the $\lambda/8$ and $\lambda/2$ coaxial lines are constructed of aluminium tubing of large diameter (O.D. 23.6 cm) so as to permit free air insulation. The inner conductors, of appropriate diameter, are supported by ceramic rods placed every 3 meters; the surface electric stress is less than 15 kV/cm.

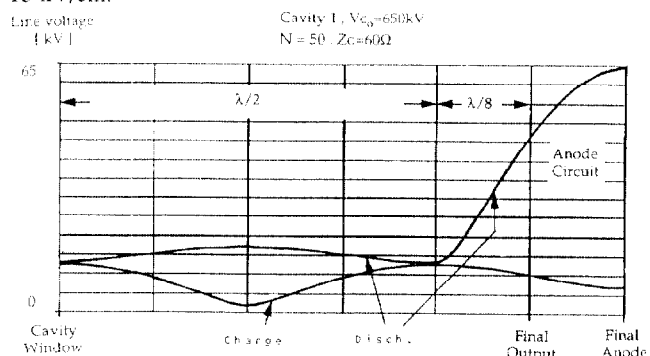


Fig. 7: Standing waves during the flat-top and discharge

During the cavity filling the rf amplitude modulation results in an image impedance at the final tube which appears to be decreasing as filling proceeds (Fig. 8). The product NZ_0 which was selected to give short discharge time, results in an anode load of about 35 Ω at the end of cavity filling. The final tube power gain is therefore low (~4 dB) and a driver power of 300 kW at cathode is necessary to maintain 700 kW at the cavity.

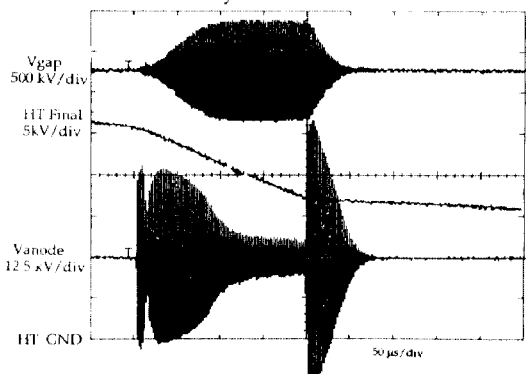


Fig. 8: Gap, anode and final HT supply voltages

The three stage driver chain with 90 dB overall gain consists of a 2 W solid state amplifier, a 1 kW narrow band tetrode amplifier and a 25 dB, 300 kW narrow band power tetrode output stage. This stage is coupled via a 50 Ω line to the 50 Ω to 4 Ω matching circuit on the final tube cathode.

During tests it was found that, without a servo system, control of V_d during the discharge was difficult. In particular, at the start of discharge even small drift of the V_d program caused excessively high voltages which triggered the tube protection spark gap. This problem was solved by employing a Metrosil non-linear resistor stack, which gave good control of V_d early in the discharge period whilst dissipating negligible power during cavity filling. Towards the end of the discharge period it was found that maximum final tube V_a cannot be maintained even with zero V_d drive, because of the low tube output impedance (~500 Ω). With the non-linear resistor in place and a simple V_d discharge program, the discharge time is 50 μ s which is greater than the desired 20 μ s but sufficient for good operation.

Servo Systems

The electrical performance of the system is stabilized by the action of 3 servo-loops (Fig. 6).

The tuning loop is of sampled type, because the speed of the tuning motors is slow compared to the duration of the rf pulse. It guarantees a resistive impedance for the final tube in stationary conditions (bunch rotation), by cancelling the phase difference between cathode and anode. For proton operation of the AC both cavities can be detuned (+15 kHz) in order to avoid instabilities of the higher intensity proton test beam.

The voltage and phase control loops are fast (15 kHz bandwidth) and active all along the pulse, except during the discharge. Low-pass networks are implemented to compensate the high-pass-like transfer function for modulation, of the amplifier + cavity assembly, due to the $\lambda/4$ driving line. Special care is taken to minimize the transient when switching from bunch rotation to discharge, and from discharge to adiabatic debunching. The operational dynamic range of voltage control (650 kV to 1 kV) results from a logarithmic envelope detector, coupled with an antilog modulator to maintain a constant open loop gain. The phase loop stabilizes the phase shift of the complete system, from the low-level drive to the gap voltage.

Stability of beam performance was greatly improved when all these loops were properly working. The quality of the controlled rf parameters can be noticed in Fig. 9.

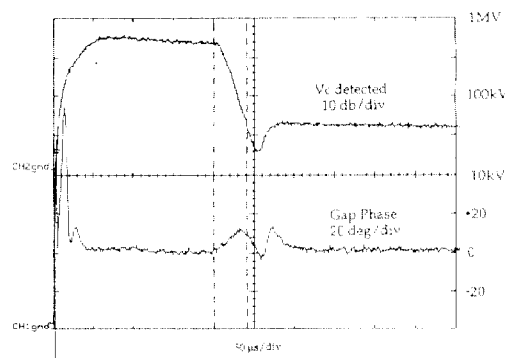


Fig. 9: Gap voltage and phase.

Operating Experience

Both cavities and associated rf generators were installed and commissioned in the AC ring by early 1988. Since then, operational experience has been very satisfactory with a total cavity voltage of 1.1 MV and discharge time of 50 μ s. Bunch rotation efficiencies of 80% are obtained with typical injected bunch length of 18 ns. The equipment failure rate is about 0.3%.

Acknowledgements

The choice of the original high power components was made by W. Pirkel. S. Talas was responsible for the cavity mechanical design. The final configuration of the high-power part of the system is mainly due to C. Zettler who also supervised the manufacture and first tests of the cavities. R. Barthelemy, W. Weissflog and S. Wynn-Werninck contributed actively to many hardware components.

References.

- [1] E.J.N. Wilson (Editor), "Design Study of an Antiproton Collector for the Antiproton Accumulator (ACOL)", PS Division, CERN 83-10, October 1983
- [2] P. Marchand, "ACOL Bunch Rotator: Cavity Design", CERN/PS/RF/Note 85-7, November 1985
- [3] G. Nassibian, "A Possible Method for Reducing the Voltage Fall Time of the ACOL Bunch Rotating Cavities", CERN/PS/RF/Note 86-1, January 1986